Uzbekistan Journal of Polymers

journal homepage: https://uzpolymerjournal.com/
ISSN (online): 2181-3256 (print) 2181-3246

CONCENTRATION DEPENDENT RHEOLOGICAL BEHAVIOR OF PAN COPOLYMER SOLUTIONS AND STRUCTURAL CHARACTERIZATION OF ELECTROSPUN FIBERS.

Turayev J.I., Ashurov N.Sh., Abdurazokov M., Shakhabutdinov S.Sh., Atakhanov A.A.

Institute of polymer chemistry and physics, Tashkent, 100128 Uzbekistan

ARTICLE INFO

Received: 11 September 2025
Revised: 07 October 2025
Accepted: 13 October 2025

Keywords:
polyacrylonitrile (PAN), rheology, nanofibers.

Corresponding author: *Turayev J.I.*
jamoliddintorayev02@gmail.com

ABSTRACT

This study establishes a direct quantitative link between rheological parameters and nanofiber structure. As the concentration increased, a significant transition from viscous to elastic-dominant behavior was observed, indicating the formation of a more interconnected polymer network. Electrospinning was subsequently used to fabricate nanofibers from the polymer solutions. The nanofibers were characterized using Fourier-transform infrared spectroscopy (FTIR), X-ray diffraction (XRD and scanning electron microscopy (SEM). FTIR spectra con-firmed the presence of characteristic PAN functional groups with minor shifts reflecting con-centration-related molecular interactions. XRD patterns revealed an increase in crystallinity with rising concentration. The main objective of this study is to determine the critical concentration regime for stable fiber formation and to correlate viscoelastic parameters with fiber structure.

Introduction

Electrospinning has emerged as a versatile and efficient technique for producing ultrafine polymeric fibers with diameters ranging from tens of nanometers to a few microme-ters [1–3]. Among the various polymers employed for electrospinning polyacrylonitrile (PAN) has gained considerable attention due to its excellent spinnability chemical resistance and role as a precursor for carbon nanofiber production [4–6]. The morphology diameter and internal structure of electrospun PAN nanofibers are critically influenced by the rheological properties of the spinning solution which are in turn highly sensitive to polymer concentration [7–9].

The concentration of PAN in solution governs not only the viscosity and viscoelastic behavior but also affects fiber formation mechanisms such as jet stability, whipping behavior and solvent evaporation dynamics during electrospinning [10–12]. At low concentrations bead formation is common due to insufficient chain entanglement [13] whereas high concentrations often yield thicker uniform fibers due to enhanced viscoelasticity [14]. The transition from dilute to semidilute and eventually to concentrated regimes profoundly alters the flow behav-ior influencing solution spinnability and the resulting fiber morphology [15–17].

Rheological characterization particularly measurements of shear and extensional viscosi-ties provides key insights into molecular interactions and chain dynamics in PAN solutions [18–20]. PAN solutions typically exhibit non-Newtonian shear-thinning behavior attributed to the alignment of polymer chains under shear stress [21]. The critical entanglement concentra-tion (Ce) marks a threshold beyond which chain entanglement dominates the flow behavior enabling fiber formation

without beads [22-23]. Accurate determination of this concentration is essential for optimizing spinning parameters and achieving desirable fiber architectures [24–26].

The solvent system also plays a pivotal role in influencing PAN solution behavior. Dimethylformamide (DMF) is widely used due to its high polarity and excellent solvation capability for PAN chains [27-28]. Variations in PAN concentration in DMF result in changes in both solution structure and interactions which manifest in the rheological and electrospin-ning performance [29-30]. Understanding this relationship is critical for tailoring fiber proper-ties such as porosity, orientation, and mechanical strength [31-32].

After electrospinning the structural characterization of PAN nanofibers is essential to link processing conditions with final fiber performance. Techniques such as scanning electron microscopy (SEM), Fourier-transform infrared spectroscopy (FTIR), and X-ray diffraction (XRD) are widely employed to assess fiber diameter distribution, surface morphology, crystal-linity and molecular orientation [33–35]. Previous studies have shown that increasing PAN concentration leads to improved fiber uniformity and higher crystallinity, thereby influencing subsequent carbonization behavior [36–38].

In addition recent studies have focused on linking the rheological properties of PAN so-lutions to the architecture and properties of electrospun fibers [39–41]. However a comprehen-sive understanding of how varying PAN concentration impacts both rheological behavior and the microstructure of resulting nanofibers remains incomplete. Particularly the need to system-atically bridge the viscoelastic features of PAN solutions with the fiber formation mechanism and final nanofiber structure motivates further in-depth investigation [42–45].

This study aims to address this gap by systematically studying the concentration-dependent rheological behavior of PAN/DMF solutions and relating these properties to the structural properties of electrospun nanofibers. Through detailed rheological analyses and morphological evaluations, we aim to identify the critical concentration regimes that govern fiber formation and to gain insight into the structure and fiber morphology of PAN-based nanofibers.

Experimental

Materials:

The objects of study were polyacrylonitrile (Navoiazot Open Joint Stock Company (Uzbekistan), molecular mass 152 кДа). N, N-Dimethylformamide (DMF) was employed as the solvent due to its high polarity and excellent solubility for PAN. PAN solutions were prepared at four different concentrations: 5 wt%, 7 wt%, 9 wt%, and 11 wt%.

Preparation of PAN Copolymer Solutions:

For each concentration the appropriate amount of PAN copolymer was added to DMF and stirred using a magnetic stirrer at stirring speed of 500 rpm. The stirring process was carried out at 60 °C for 24 hours to ensure complete dissolution of the polymer. After mixing all solutions were left to rest for 1 hour at room temperature to eliminate bubbles and allow for structural relaxation before electrospinning.

Rheological process:

The behavior of solutions was studied in a shear flow generated in a system of coaxial cylinders of an Anton Paar modular compact rheometer MCR 92 at temperatures of 25, 30, 35, 40, 45, 50, and 55°C. Rheological data were processed using the RheoCompass software.

Electrospinning Process:

The electrospinning of PAN solutions was performed under ambient room temperature conditions. A high-voltage power supply of 20 kV was applied to initiate the spinning process. The distance between the needle tip and the collector was maintained at 12 cm. A 23G stainless steel needle was used and the flow rate of the polymer solution was set to 14 μL/min. The fibers were collected on a flat aluminum foil covered collector for subsequent analysis.

FTIR analysis:

IR spectroscopy studies were performed using a Bruker Inventio-S Fourier-transform IR instrument in the wave num ber range from 400 to 4000 cm^{-1} with a resolution of 4 cm^{-1}, a signal: noise ratio of 30 000:1, and a scanning speed of 16 spectra per second.

X-ray analysis:

X-ray diffraction studies were carried out using a Rigaku Miniflex 600 diffractometer with monochromatic CuKα radiation with a wavelength λ = 1.5418 Å at a voltage of 40 kV and a current of 15 mA. The samples were studied in the form of nonwoven materials. The measurement was carried out in the angle range of 2θ = 2°– 40°. Diffraction patterns were processed
using the SmartLab Studio II software; fixed slits having an angle of 1.25° were used. Experiments were carried out in reflection (Bragg–Brentano) mode using the Rietveld method and the pseudo-Voight function.

Results and discussion

The dissolution of highly polar polymers in highly polar solvents occurs by breaking polar-polar bonds between the polymers and then forming new polar-polar bonds between the polymer and the solvent. It took 26 and 57 minutes to dissolve the PAN samples in DMF and DMSO, respectively. This means that DMF dissolves PAN 2.19 times faster than DMSO [46-47].

Based on the experimental observation, the dissolution mechanism of PAN in DMF proposed in Scheme 1. Solvent molecules first penetrate into polymer chains under the dominant influence of the entropic effect and break up the physical bonds between the polymers. Then, the physical bonds between polymer and solvent molecule are newly formed, in which the enthalpic effect is dominant. The strong polar nitrile group of PAN would polarize the solvent molecules, leading to the orientation of the polarized solvent molecules.
This results in the formation of a solvent bridge as shown in Scheme 1. It should be noted that the nitrile groups would have a strong polarizing effect on the solvent molecules because they are isolated by carbon-carbon single bond backbone which does not permit the electron density fluctuation. The process is analogous to associative interactions rather than chemical SN2-type reactions.

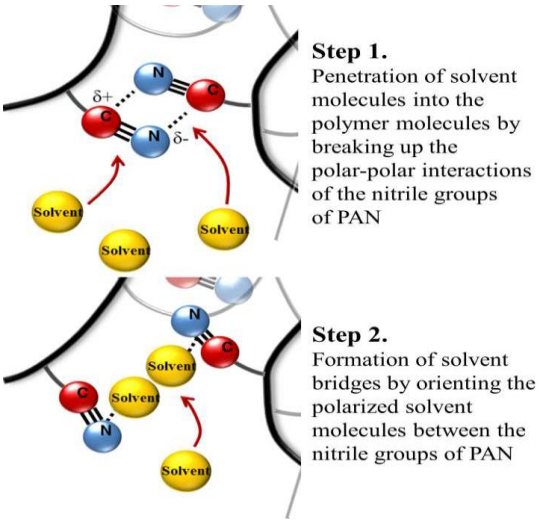

Scheme 1. *Schematic diagram of the dissolution mechanism of PAN in DMF; carbons are shown in red, nitrogens in blue, and solvent molecules in yellow*

The intrinsic viscosity ([η]) of PAN solutions was calculated using the Solomon-Ciuta equation of a single point measurement the intrinsic viscosity ([η]) of PAN solutions in DMF is given in Table 1.

$$[\eta] = [2*(\eta_{sp} - \ln\eta_{rel})]^{1/2} /c \qquad (1).$$

The rheological characterization of PAN copolymer solutions with varying concentrations (5%, 7%, 9%, and 11%) in DMF was performed to evaluate their viscoelastic properties and determine the suitability of the solutions for fiber formation via electrospinning [45-48].
The zero-shear viscosity (η_0) exhibited a pronounced increase with polymer concentration rising from 1020.0 mPa·s at 5% to 3590.9 mPa·s at 11% (Fig. 1.). This significant growth indicates intensified polymer chain entanglement at higher concentrations, which is a prerequisite for continuous fiber formation

Table 1.

Viscosity properties of PAN copolymer dissolved in DMF at various concentrations

№	C %	η_0 (mPa s)	η_{sp}	η_{rel}	[η] (dL/g)
1	5	1020.0	1274.0	1275.0	100.67
2	7	1489.1	1861.6	1861.4	672.7
3	9	2963.1	3702.9	4628.6	860.2
4	11	3590.9	4487.6	5120.0	955.1

The relative viscosity (η_{rel}) also showed a non-linear increase from 1275.0 to 5120.0 This suggests a sharp rise in flow resistance due to enhanced hydrodynamic volume and molecular interactions, particularly above 7% where the solution behaves more like a viscoelastic gel than a Newtonian fluid.

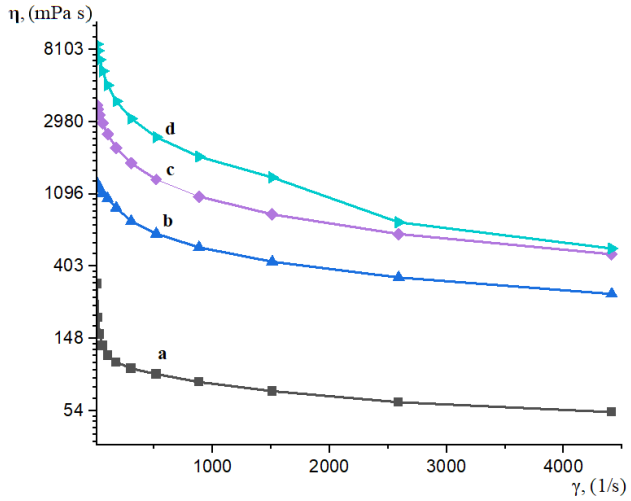

Figure 1. *η of the PAN copolymer solutions as a function of the shear rate at various concentrations (1-from bottom to top) a) PAN 5%, b) PAN 7%, c) PAN 9% and d) PAN 11%*

The intrinsic viscosity ([η]) which reflects the hydrodynamic volume and molecular conformation of the polymer in solution, increased significantly from 100.67 to 955.1 dL/g. This increase confirms the expansion of polymer coils and strong intermolecular interactions at higher concentrations, contributing to a more elastic and stable solution structure. Overall the observed rheological parameters suggest that PAN copolymer solutions exhibit concentration-dependent non-Newtonian behavior. Above 7% the solutions attain sufficient viscoelasticity and chain entanglement necessary for fiber formation during electrospinning, making them ideal candidates for nanofiber production [49-50].

Typically, the viscoelastic behavior of a polymer solution with respect to temperature can be investigated using the loss tangent (tan δ). The time-dependent viscoelastic behavior was measured at a constant low frequency of 10 rad/s. Gelation is defined as the point where the storage modulus (G′) and loss modulus (G″) intersect, indicating a transition to solid-like behavior. This occurs when tan(δ) = 1, where the ratio between G′ and G″ becomes equal, marking the onset of gelation. Therefore, the gelation point can be expressed by the following Equation (2) [53–58].

$$G' = G'' \qquad (2)$$

In principle, when tan (δ) is greater than 1, a liquid-like viscosity is exhibited, whereas a solid-like viscosity is dominant when tan (δ) is less than 1. The tan (δ), as well as G′ for each temperature and frequency, are shown in Figure 1. Regardless of the moisture content, all samples showed liquid-like viscous properties in the initial state and sol–gel transition regions. For PAN solutions, tan δ > 1 in all tested concentrations, indicating viscous-dominant behavior. The gradual reduction of tan δ with increasing concentration suggests enhanced elasticity and the approach to gel-like behavior. [20-26]. For all samples, the complex viscosity (η*) gradually increased with increasing time. However, there were some minor differences with respect to moisture content.

All experiments show that the viscosity and shear strength of the solutions were affected by the increase in the concentration of the PAN copolymer. It has been reported that morphology such as fiber diameter and its uniformity of the as-pun polymer fibers are linked to many processing parameters. However, many researchers have highlighted that under certain conditions, not only uniform fibers but also beads-free fibers could be fabricated. Therefore, in this paper so as to obtain beads-free and uniform PAN nanofibers, different electrospinning solutions with different PAN contents (5, 7, 9 and 11 wt. % by mass) were prepared and electrospun at 20 kV, respectively. The morphology of the as-fabricated PAN nanofibers was characterized by SEM and their respective results were displayed in (Fig. 2.). It was observed that even though at 5 wt. % of PAN, nanofibers with smaller average diameters were obtained but an important number of spindle-like beads were visible as well. The electrospinning of solutions containing a PAN content higher than 5wt. % led to the fabrication of fibers without beads. It is worth noting that at 11 wt. % of PAN, branched fibers were observed. The formation of branched fibers can be justified by the instability of the jet due to the discrepancy between the electrical forces and surface tension. It was reported that such instability can decrease its local charge per unit surface area by ejecting a smaller jet from the surface of the primary jet or by splitting apart into two smaller jets [51-55]. In 7 and 9 wt. % of PAN uniform nanofibers without any spindle-like beads were obtained. In addition, it was observed that increasing the PAN concentration, generally led to the increase of the fibers average diameter.

As polymer concentration increases, enhanced chain entanglement suppresses jet instability, leading to better molecular alignment along the electrospinning direction, which in turn promotes crystallization during solvent evaporation..

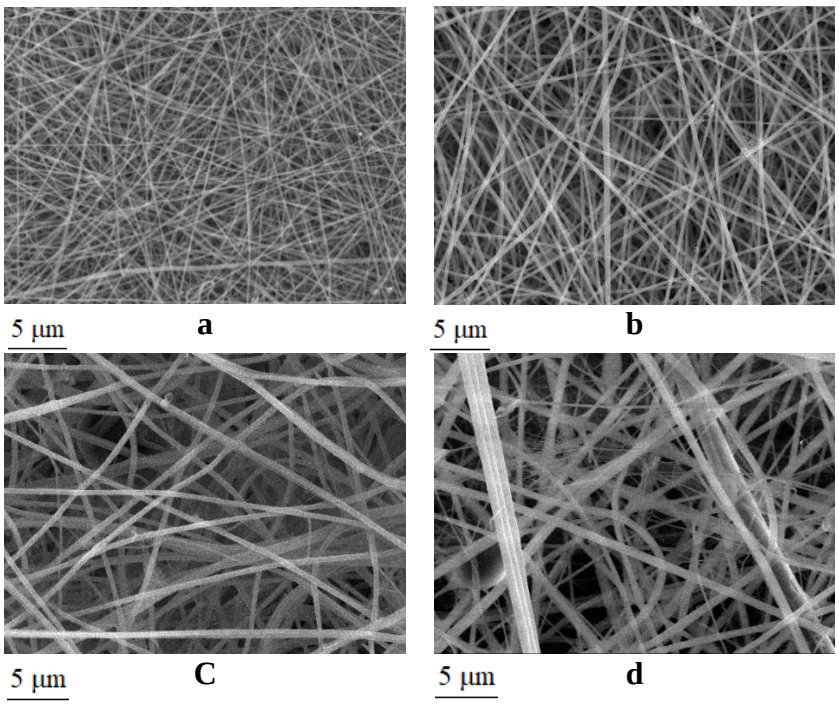

Figure 2. *Scanning electron micrographs of electrospun PAN copoly-mer fibers at various concentrations. a) PAN 5%, b) PAN 7%, c) PAN 9% and d) PAN 11%*

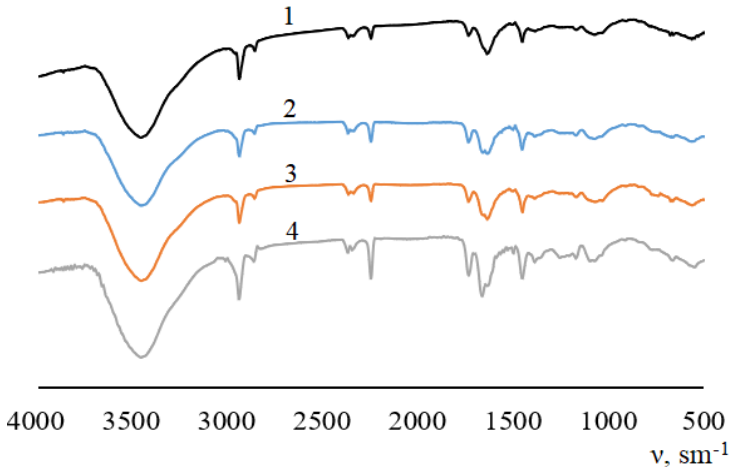

Figure 3. *FTIR spectra of PAN copolymer nanofibers 1) PAN 5%, 2) PAN 7%, 3) PAN 9% and 4) PAN 11%*

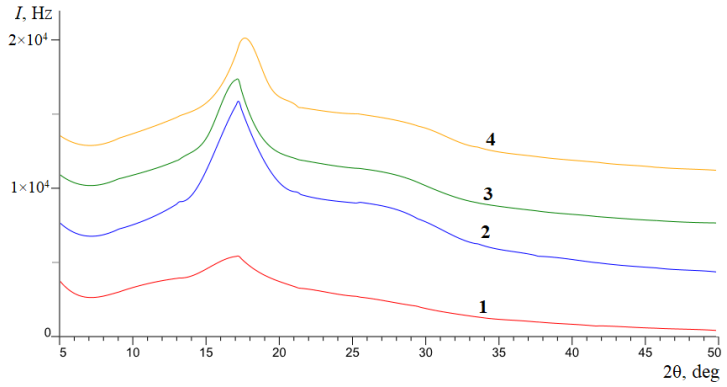

Figure 4. *X-ray diffraction patterns of PAN copolymer nanofibers 1) PAN 5%, 2) PAN 7%, 3) PAN 9% and 4) PAN 11%*

FTIR spectra of PAN copolymer nanofibers synthesized with concentrations of 5%, 7%, 9%, and 11% (Fig. 3.). The spectra, recorded in the 4000–500 cm^{-1} range display the characteristic absorption bands of polyacrylonitrile (PAN) confirming the retention of key functional groups across all samples. The prominent absorption peak observed near 2240–2250 cm^{-1} corresponds to the stretching vibration of the nitrile (–C≡N) group which is the signature band of PAN. The intensity of this band increases slightly with concentration indicating a higher density of nitrile groups and possibly enhanced molecular orientation in higher concentration samples. The bands located around 1450–1470 cm^{-1} are attributed to the bending vibrations of $–CH_2–$ groups, while the 1360–1380 cm^{-1} range corresponds to –CH bending. These confirm the hydrocarbon backbone of the PAN copolymer. Several peaks appearing in the 1050–1300 cm^{-1} region represent the C–H and C–C stretching and bending vibrations indicating the complex chain structure of the copolymer. A broad and weak band in the 3500–3300 cm^{-1} range suggests the presence of O–H stretching likely due to moisture absorption or intermolecular hydrogen bonding. Its intensity slightly increases in higher concentration samples suggesting increased moisture retention due to denser fiber structure.

X-ray diffraction analysis showed that the diffraction patterns of PAN copolymer nanofibers with varying concentrations (5%, 7%, 9%, and 11%) are shown in (Fig. 4). A prominent broad diffraction peak centered at approximately $2\theta \approx 17°$ is observed for all samples corresponding to the (100) plane of PAN. This peak is indicative of the semi-crystalline nature of PAN nanofibers.

A gradual increase in diffraction intensity and sharpening of the peak is observed as the PAN concentration increases from 5% to 11%. The 5% PAN nanofiber exhibits a weak and broad peak, signifying a largely amorphous structure with minimal molecular ordering. With 7% PAN, the peak becomes more defined, suggesting the onset of crystallization. As the concentration reaches 9% and 11%, the intensity increases substantially, indicating improved chain alignment and molecular ordering during electrospinning. The 11% PAN sample displays the most intense and sharpest peak, signifying a higher degree of crystallinity. These results confirm that polymer chain interactions and structural ordering are strongly dependent on concentration [56-57].

Conclusions

In this study, the concentration-dependent rheological behavior of PAN copolymer solutions and the structural characteristics of electrospun nanofibers were thoroughly investigated. Rheological analysis revealed that increasing the PAN concentration leads to a non-linear enhancement in viscosity, intrinsic viscosity and viscoelastic moduli indicating stronger chain entanglements and the formation of a more stable network.

FTIR analysis confirmed the preservation of PAN's characteristic functional groups across all concentrations with minor shifts associated with intermolecular interactions. XRD patterns showed a clear trend of increasing crystallinity as concentration increased suggesting improved molecular ordering in the electrospun fibers.

Morphological analysis demonstrated that bead-free and uniform fibers are obtained at concentrations above 5%, with optimal fiber formation at 7% and 9%. However, excessive concentration (11%) caused jet instability leading to branched fiber formation.

The identified concentration window (7–9 wt%) can be used for stable electrospinning of PAN precursors for subsequent carbon fiber production the critical role of polymer concentration in determining the rheological behavior, molecular interactions and structural integrity of electrospun PAN nanofibers. The results provide valuable insights for optimizing solution preparation and processing conditions in nanofiber fabrication.

REFERENCES

[1]. Li, D., Xia, Y. Adv. Mater., 2004, 16, 1151–1170. https://doi.org/10.1002/adma.200400719

[2]. Ramakrishna, S., et al. Mater. Today, 2005, 8, 40–50. https://doi.org/10.1142/9789812567611_0003

[3]. Bhardwaj, N., Kundu, S.C. Biotechnol. Adv., 2010, 28, 325–347. https://doi.org/10.1016/j.biotechadv.2010.01.004

[4]. Doshi, J., Reneker, D.H. J. Electrostat., 1995, 35, 151–160. http://dx.doi.org/10.1016/0304-3886(95)00041-8

[5]. Liu, Y., Kumar, S. Polymer, 2005, 46, 4799–4810. https://doi.org/10.1021/jp201077p

[6]. Rutledge, G.C., Fridrikh, S.V. Adv. Drug Deliv. Rev., 2007, 59, 1384–1391. https://doi.org/10.1016/j.addr.2007.04.020

[7]. Sill, T.J., von Recum, H.A. Biomaterials, 2008, 29, 1989–2006. https://doi.org/ 10.1016/j.biomaterials.2008.01.011

[8]. Fong, H., et al. Polymer, 1999, 40, 4585–4592. https://doi.org/10.1016/S0032-3861(99)00068-3

[9]. https://doi.org/10.1016/j.polymer.2007.09.017

[10]. Barnes, H.A., J. Non-Newtonian Fluid Mech., 1997, 70, 1–33. https://doi.org/10.1016/S0377-0257(97)00004-9

[11]. Shenoy, S.L., et al. Polymer, 2005, 46, 3372–3384.

[12]. https://doi.org/10.1016/j.polimer.2005.03.011

[13]. Deitzel, J.M., et al. Polymer, 2001, 42, 261–272. https://doi.org/10.1016/S0032-3861(00)00250-0

[14]. Tripatanasuwan, S., et al. Polymer, 2007, 48, 5742–5751.

[15]. Jaworek, A. J. Mater. Sci., 2007, 42, 266–297. https://doi.org/10.1007/978-3-319-49869-0_1

[16]. He, J.H., et al. J. Appl. Polym. Sci., 2006, 99, 364–372.

[17]. McKee, M.G., et al. Macromolecules, 2004, 37, 1760–1767. https://doi.org/10.1021/ma035689h
[18]. Barnes, H.A., J. Non-Newtonian Fluid Mech., 1994, 56, 221–251.
[19]. Larrondo, L., Manley, R.S.J. J. Polym. Sci. Polym. Phys. Ed., 1981, 9, 909–920. https://doi.org/10.1002/pol.1981.180190601
[20]. Ziabari, M., et al. J. Appl. Phys., 2006, 100, 074906.
[21]. Lin, L., et al. Polymer, 2009, 50, 1853–1861. https://doi.org/10.1016/j.polymer.2007.09.017
[22]. Abdalrahem, M.A., et al. Polym. Bull., 2019, 76, 251–265.
[23]. Martins, C.A., et al. J. Non-Newtonian Fluid Mech., 2021, 290, 104519.
[24]. Demir, M.M., et al. Polymer, 2002, 43, 3303–3309. https://doi.org/10.1016/S0032-3861(02)00136-2
[25]. Yousefi, N., et al. Carbon, 2013, 59, 406–417. DOI: 10.1039/C5RA13897C
[26]. Huang, Z.-M., et al. Compos. Sci. Technol., 2003, 63, 2223–2253. https://doi.org/10.1016/S0266-3538(03)00178-7
[27]. Ruan, G., et al. ACS Nano, 2009, 3, 1683–1688. https://doi.org/10.1021/nn9010939
[28]. Lu, X., et al. Polymers, 2013, 5, 1169–1180. https://doi.org/10.3390/polym5041169
[29]. Jing, X., et al. Mater. Lett., 2015, 142, 273–276. https://doi.org/ 10.1002/smll.201002009
[30]. Ma, Z., Kotaki, M., Ramakrishna, S. J. Membr. Sci., 2005, 265, 115–123. https://doi.org/ 10.1007/s10570-012-9734-0
[31]. Agarwal, S., et al. Prog. Polym. Sci., 2013, 38, 963–991. https://doi.org/10.1016/j.progpolymsci.2013.02.001
[32]. Shin, Y.M., et al. Appl. Phys. Lett., 2001, 78, 1149–1151. https://doi.org/ 10.1089/ten.2006.12.1197
[33]. Saito, Y., et al. Polymer J., 2003, 35, 178–182. https://doi.org/10.1002/0471532053.bra049
[34]. Zhang, C., et al. Polymer, 2009, 50, 2087–2093.
[35]. Eom Y. and Kim B. Ch. (2014). Solubility Parameter-Based Analysis of Polyacrylonitrile Solutions in *N*,*N*-Dimethyl Formamide and Dimethyl Sulfoxide https://doi.org/10.1016/j.polymer.2014.03.047
[36]. Youngho E., Hyejin J., Yeonju P., Dong W.Ch., Young M.J., Byoung Ch. K., Han G. Ch. (2020) Effect of dissolution pathways of polyacrylonitrile on the solution homogeneity: Thermodynamic or kinetic-controlled dissolution https://doi.org/10.1016/j.polymer.2020.
[37]. Jaymin V.S., Inga L., Kanukuntala S.P., Smogor H., Gudmona A.V., Krasnikovs A., Tipans I and Gobins V. Mechanical and Thermal Characterization of Annealed Oriented PAN Nanofibers
[38]. https://doi.org/10.3390/polym15153287
[39]. Sanchaniya J.V and Kanukuntla S. (2023) Morphology and mechanical properties of PAN nanofiber mat https://doi.org/10.1088/1742-6596/2423/1/012018
[40]. Thenmozhi S., Dharmaraj N., Kadirvelu K., Kim H.Y. (2017) Electrospun Nanofibers: New Generation Materials for Advanced Applications. Mater. Sci. Eng. B Solid-State Mater. Adv. Technol. 2017, 217, 36–48. [Google Scholar] [CrossRef]
[41]. Merighi S., Mazzocchetti L., Benelli T., Maccaferri E., Zucchelli A., D'Amore A., Giorgini L. A. (2019) New Wood Surface Flame-Retardant Based on Poly-m-Aramid Electrospun Nanofibers. Polym. Eng. Sci. 2019, 59, 2541–2549. [Google Scholar] [CrossRef].
[42]. Maccaferri E., Mazzocchetti L., Benelli T., Brugo T.M., Zucchelli A., Giorgini, L. (2021) Rubbery-Modified Cfrps with Improved Mode i Fracture Toughness: Effect of Nanofibrous Mat Grammage and Positioning on Tanδ Behaviour. Polymers 2021, 13, 1918. [Google Scholar] [CrossRef] [PubMed]
[43]. Quan Z., Xu Y., Rong H., Yang W., Yang Y., Wei G. (2022) Preparation of Oil-in-Water Core-Sheath Nanofibers through Emulsion Electrospinning for Phase Change Temperature Regulation. Polymer 2022, 256, 125252. [Google Scholar] [CrossRef]
[44]. Tipduangta P., Belton P., Fábián L., Wang L.Y., Tang H., Eddleston M., Qi, S. (2016) Electrospun Polymer Blend Nanofibers for Tunable Drug Delivery: The Role of Transformative Phase Separation on Controlling the Release Rate. Mol. Pharm. 2016, 13, 25–39. [Google Scholar] [CrossRef]
[45]. Balaganesh D., Neeraja B., Kalaivizhi R. (2024) Electrospun polyacrylonitrile-based nanofibrous membrane for various biomedical applications https://doi.org/10.1007/s10965-024-03965-x

[46]. Yuan G., Zhongyu F., Yunjiao D., Mingyao Zh., and Huixuan Zh. (2019) The effects of chemical reaction on the microstructure and mechanical properties of polyacrylonitrile (PAN) precursor fibers https://doi.org/10.1007/s10853-019-03781-5

[47]. Sharifah Sh., Syed B., Kar M.F., Norzilah A.H and Shuhaida Y. (2018) Effect of solution concentration and applied voltage on electrospun polyacrylonitrile fibers https://doi.org/10.1088/1757-899X/701/1/012018

[48]. Jian H., Feng A., Chunxiang L., and Yaodong L. (2019) Solvent effects on radical copolymerization of acrylonitrile and methyl acrylate: solvent polarity and solvent-monomer interaction https://doi.org/10.1080/10601325.2019.1642767

[49]. Skvortsov I.Y., Chernikova E.V., Kulichikhin V.G., Varfolomeeva L.A., Kuzin M.S., Toms R.V and Prokopov N.I. (2020) The Effect of the Synthetic Procedure of Acrylonitrile–Acrylic Acid Copolymers on Rheological Properties of Solutions and Features of Fiber Spinning https://doi.org/10.3390/ma13163454

[50]. Skvortsov I.Y., Maksimov N.M., Kuzin M.S., Toms R.V., Varfolomeeva L.A., Elena Chernikova V and. Kulichikhin V.G (2023) Influence of Alkyl Acrylate Nature on Rheological Properties of Polyacrylonitrile Terpolymers Solutions, Spinnability and Mechanical Characteristics of Fibers https://doi.org/10.3390/ma16010107

[51]. Varfolomeeva L.A., Skvortsov I.Y., Kuzin M.S and Kulichikhin V.G. (2022) Polyacrylonitrile Solutions: Rheology, Morphology, Coagulation, and Fiber Spinning https://doi.org/10.3390/polym14214548

[52]. Porkodi P., Abhilash J. K., Hemant K.Sh., Jaya R. (2020) Rheological properties of concentrated polyacrylonitrile co-polymer and lignin blend solution https://doi.org/10.1007/s00289-019-02944-3

[53]. Golovaa L. K., Makarova I. S., Vinogradova M. I., Kuznetsova L. K., and Kulichikhina V.G. (2018) Morphological Features and Rheological Properties of Combined Cellulose and Polyacrylonitrile Solutions in N-Methylmorpholine-N-oxide https://doi.org/10.1134/S0965545X18060056

[54]. Wenlong X., Binjie Xi., Xue Y. (2020) Carbonization of electrospun polyacrylonitrile (PAN)/cellulose nanofibril (CNF) hybrid membranes and its mechanism https://doi.org/10.1007/s10570-020-03006-y

[55]. Ryšáneka P., Benadaa O., Tokarskýc J., Syrovýa M., Čapkováa P., Pavlíka J. (2019) Specific structure, morphology, and properties of polyacrylonitrile (PAN) membranes prepared by needleless electrospinning; Forming hollow fibers needle https://doi.org/10.1016/j.msec.2019.110151

[56]. Park D.U., Ryu J.H., Han N.K., Park W.H and Jeong Y.G. (2018) Thermal Analysis on the Stabilization Behavior of Ternary Copolymers Based on Acrylonitrile, Methyl Acrylate and Itaconic Acid https://doi.org/10.1007/s12221-018-8782-y

[57]. Atakhanov A.A., Ashurov N.Sh., Turaev J.I., Abdurazakov M., Ashurova N. R., Rashidova S. Sh., and Berlinb A. A. (2024) Formation of Nanofibers Based on Polyacrylonitrile with Graphite and Their Structural Characteristics Published: 31 May 2024 Vol 66, pages 81–87.